

Fortgeschrittenen-Praktikum II
Albert-Ludwigs-Universität Freiburg

Report
Compton Scattering

Isabelle Schmager Frank Sauerburger

24. - 28. February 2014

isabelle@schmager.com
frank@sauerburger.net

Tutor: Phuong Dang

Contents

1	Introduction	2
2	Theoretical Background	3
2.1	Radioactive Sources	3
2.2	COMPTON Scattering	3
2.3	Scintillator	5
2.3.1	Organic Scintillator	5
2.3.2	Inorganic Scintillator	5
2.4	Cross Section	6
3	Setup and Measurement Procedure	7
3.1	Setup	7
3.2	Measurement Procedure	8
3.2.1	Delay Setting	8
3.2.2	Energy Calibration	8
3.2.3	Conservation of Energy and Differential Cross Section	8
3.2.4	Background an Random Coincidence	8
4	Analysis	9
4.1	General Assertion of Statistical Error	9
4.2	Energy Calibration	10
4.2.1	Inorganic Scintillator	10
4.2.2	Organic Scintillator	11
4.3	Conservation of Energy	13
4.4	Differential Cross Section	15
4.5	Discussion of Errors	18
5	Conclusion	19
A	Appendix	20
A.1	Settings	20
A.2	Energy Calibration	20
A.3	Conservation of Energy	23
A.3.1	Organic Scintillator	23
A.3.2	Anorganic Scintillator	26
A.4	Cross Section	29
A.5	Notes	29
	References	34

1 Introduction

Until 1922, when ARTHUR COMPTON discovered the so called COMPTON effect, the photo electrical effect was the only proof of the wave particle dualism which ALBERT EINSTEIN had postulated in 1905. COMPTON discovered the characteristic scattering angle distribution and then realized that the scattered light had less energy depending on the scattering angle. He showed that his phenomena can be explained by an elastic scattering of electron and photon.

In our experiment we want to

- (A) verify the conservation of energy and
- (B) measure the differential cross section of COMPTON scattering.

2 Theoretical Background

The following sections will give an overview of topics which are necessary to explain the COMPTON effect and our equipment we use to measure the effect.

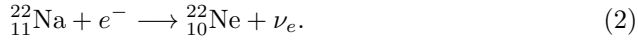
2.1 Radioactive Sources

In our experiment we use two different sources of radiation ^{22}Na and ^{137}Cs .

Sodium-22 [1]: We use ^{22}Na for the energy calibration and to set the delays. The ^{22}Na isotope undergoes a beta (β^+) decay as illustrated in equation (1).



A proton of the sodium decays to a neutron and the sodium therefore becomes neon. To account to conservation of charge and lepton number a positron e^+ and an electron neutrino ν_e is emitted. The life time of ^{22}Na is 2.6 years. The positron annihilates with surrounding electrons which creates two photons with an energy of 511keV each. The produced neon is in an excited state which returns to the ground state in a lifetime of 5ps under emission of a photon with an energy of 1275keV. It is also possible that the sodium undergoes electron capture



An electron from the K shell interacts with a proton of the nucleus which becomes a neutron by emission of an anti-electron neutrino. Other electrons fill the hole in the K shell and thereby emit a photon. The electron capture is ten times less likely than beta decay.

Cesium-137 [2]: We use ^{137}Cs for the energy calibration, to show the conservation of energy and to measure the differential cross section. The ^{137}Cs isotope undergoes a beta (β^-) decay



A neutron of the cesium decays to a proton and the cesium therefore becomes barium. To account to the conservation of charge and lepton number an electron e^- and an anti-electron neutrino $\bar{\nu}_e$ is emitted. The life time of ^{137}Cs is 30 years. The produced barium is in an excited state which returns to the ground state in a lifetime of 2.5min under emission of a photon with an energy of 661.7keV. We will use these photons for our experiment.

2.2 Compton Scattering

The COMPTON scattering is an elastic scattering of a free electron and a photon. Due to the photon we have to do a relativistic calculation. Let us assume that the

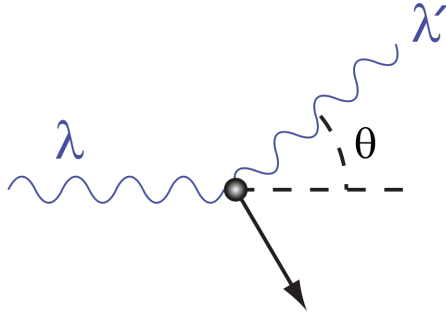


Figure 1: Illustration of the COMPTON scattering. Source [3].

electron with mass m_e is at rest and the incoming photon γ has the wavelength $\lambda = \frac{h}{E_\gamma}$ (we choose an unit system with $c = 1$). See figure 1. The relativistic four-momenta in the lab system are

$$p_\gamma = \begin{pmatrix} E_\gamma \\ E_\gamma \cdot \mathbf{e}_z \end{pmatrix}, \quad p_e = \begin{pmatrix} m_e \\ \mathbf{0} \end{pmatrix}, \quad p'_\gamma = \begin{pmatrix} E'_\gamma \\ E'_\gamma \cdot \mathbf{e}_f \end{pmatrix} \quad (4)$$

where the primed quantities correspond to the quantities after the scattering. The unit (three-)vectors \mathbf{e}_z and \mathbf{e}_f enclose the scattering angle θ , so $\mathbf{e}_z \cdot \mathbf{e}_f = \cos \theta$. We do not need to introduce the four-vector of the scattered electron. The total energy is conserved, therefore

$$p_\gamma + p_e = p'_\gamma + p'_e \quad (5)$$

$$\implies (p_\gamma + p_e - p'_\gamma)^2 = p'_e^2. \quad (6)$$

Evaluating the square and using the invariant square of the four-vectors $p_\gamma^2 = p'_\gamma^2 = 0$ and $p_e^2 = p'_e^2 = m_e$, equation (6) yields

$$p_\gamma p_e = p_e p'_\gamma + p_\gamma p'_e \quad (7)$$

$$\stackrel{(4)}{\iff} E_\gamma m_e = E'_\gamma m_e + E_\gamma E'_\gamma - E_\gamma E'_\gamma \cos \theta \quad (8)$$

From (8) we can solve for E'_γ and get

$$E'_\gamma = \frac{E_\gamma}{1 - \frac{E_\gamma}{m_e}(1 - \cos \theta)} \quad (9)$$

or we can plug in $E = \frac{h}{\lambda}$ and solve for the wavelength shift

$$\lambda' - \lambda = \frac{h}{m_e}(1 - \cos \theta) \quad (10)$$

which is the famous result that COMPTON derived. From (9) we can calculate the energy of the scattered electron

$$E'_e = E_\gamma - E'_\gamma = E_\gamma \cdot \left(1 - \frac{1}{1 - \frac{E_\gamma}{m_e}(1 - \cos \theta)} \right) \quad (11)$$

Besides COMPTON scattering there are other interactions of light with matter. Photons can decay into an electron-positron pair, what is called pair production. For that, the photons need to have at least an energy of $E = 2 \cdot m_e = 1.022\text{MeV}$. The photons from the ^{137}Cs source do not have enough energy to produce these pairs. An other interaction is called photo electrical effect. Here the photon ionizes an atom. According to [4] COMPTON scattering is the most dominant effect for photons with $E = 662\text{keV}$. We will compensate the influence of the photo electrical when we calculate the differential cross section.

2.3 Scintillator

Scintillators are used to detect ionizing radiation, utilizing that certain organic and inorganic materials emit light, when exposed to radiation. This light can be detected with a photomultiplier. In general a scintillator consists of a scintillating material and a photomultiplier.

2.3.1 Organic Scintillator

Organic scintillators are made of organic materials, the one in our experiment is a PVC scintillator. The scintillating material absorbs photons or charged particles what causes excites molecules. When the molecules relax, they emit light. There are added wave length shifters, to make the scintillator transparent for the scintillation light.

In our experiment the COMPTON scattering takes place inside the organic scintillators. The scattered electrons are detected here, whereas the scattered photons are supposed to leave the organic scintillator.

2.3.2 Inorganic Scintillator

Inorganic scintillators are contaminated crystals. Here the ionized radiation produces electron-gap pairs, which operate as charge carrier. When they fall back into the ground state, they emit light. At some places the conduction band is deformed, what changes the energy level. This makes the scintillator transparent for the scintillator light.

We use a sodium iodide (NaI) scintillator, to detect the photons, which are scattered inside the plastic scintillator.

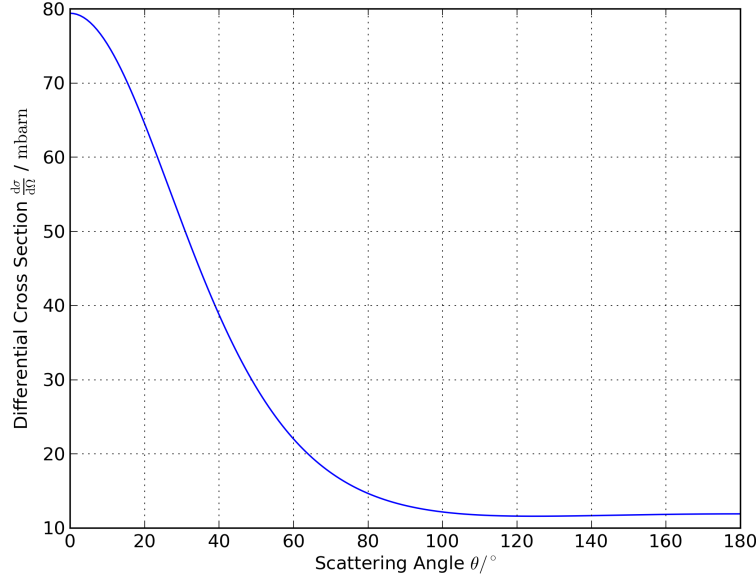


Figure 2: Dependence of differential cross section and scattering angle.

2.4 Cross Section

The cross section describes the probability that an interaction takes place. The total cross section states the probability that an interaction takes place in general, the differential cross section, the one we will measure in our experiment, states the probability that an interaction takes place in a defined solid angle.

The cross section depends on the energy of the scattered and scattering particles and on the impact parameter. For COMPTON scattering the theoretical differential cross section can be expressed with the KLEIN-NISHINA formula

$$\frac{d\sigma}{d\Omega} = \frac{1}{2} r_e^2 E'_\gamma(\theta) (1 - E'_\gamma(\theta) \sin^2(\theta) + E'_\gamma(\theta)). \quad (12)$$

E'_γ is the same as in equation (9). For further information on this see [5]. The differential cross section is shown in figure 2. The KLEIN-NISHINA formula is to be verified in our experiment.

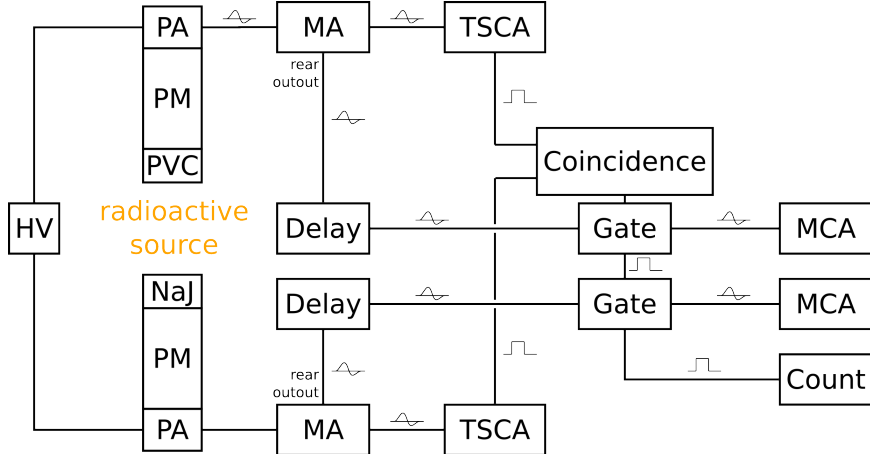


Figure 3: Schematic of our measurement setup.

3 Setup and Measurement Procedure

We will now explain our experimental setup and then explain what we measured.

3.1 Setup

There are two scintillators, a NaI scintillator and a PVC scintillator, see figure 3. Each is connected to its photomultiplier, preamplifier and main amplifier. The main amplifiers outputs are connected to delay units and to timing single channel analyzers (TSCAs). The TSCAs are connected to a coincidence unit. The coincidence unit opens two linear gates, which connect the TSCAs and multichannel analyzers (MCA). For monitoring purposes we sometimes connected the coincidence units output to a counter.

The TSCAs convert the analogous pulses into digital ones, if the pulse height is inside certain limits, called windows. These digital pulses can be delayed. The coincidence unit checks the simultaneity of the signals from both TSCAs. To ensure that the signals of two simultaneous registered events are arrive at the same time in the coincidence unit, one must consider that the cables have the same length. For that we observed our signals at the oscilloscope and adjusted delays so that the signals were coincidence. If the two digital pulses arrive at the same time, the coincidence unit opens the two linear gates (one internal and one external). The analogues signals from two simultaneously registered events are then processed by the multichannel analyzer. The multichannel analyzer is an impulse level analyzer. He distributes the impulses, depending on their voltage level, to different channels. This setup allows us to measure the spectrum of coincident events only. In our case the scattered electron in the PVC scintillator and the scattered photon in the NaI scintillator are detected at the same time.

3.2 Measurement Procedure

3.2.1 Delay Setting

First of all we arranged the setup with all devices and adjusted the delays for the scintillators. To do this, we placed the ^{22}Na source in the center of both scintillators to compare all the signals (TSCA outputs and analogous delayed signals) with the oscilloscope. The annihilation photons from the beta decay are detected simultaneously. This allows us to set the delays. The two digital TSCA signals must arrive at the same time to trigger the coincidence unit, and the two analogous delayed signals must arrive when the two linear gates are open. Our settings are in the appendix, table 4 and 5. It is important to set the delays with all devices implemented before making the energy calibration. If the delay and coincidence equipment had been installed after the energy calibration, the calibration would be void, because the additional equipment alters the analogous signal what results in energy shifts in later measurements.

3.2.2 Energy Calibration

Before starting our measurement we made the energy calibration. For that we record the direct γ spectrum of ^{22}Na and ^{137}Cs with both scintillators. The energy of characteristic peaks in these spectra are known, what allows us to gauge the channel axis.

3.2.3 Conservation of Energy and Differential Cross Section

For different scattering angles θ we recorded the electron (PVC) and photon spectrum (NaI) for coincident events produced by COMPTON scattering in the PVC scintillator. The radiation source is ^{137}Cs . This allows us to test the conservation of energy. We have measured for $\theta = 0^\circ$ through 120° in 15° steps. The measurement duration was $t = 3600\text{s}$ each.

The last part was to measure the differential cross section and to compare it with the KLEIN-NISHINA formula. We can use the data from the previous measurement to determine the scattered photon intensities. To determine the primary photon intensity, i.e. the intensity of the unshielded ^{137}Cs source, we have measured the ^{137}Cs source (without the PVC scintillator blocking the radiation) with the NaI scintillator for $t = 3600\text{s}$.

3.2.4 Background an Random Coincidence

Over the nights we measured the background and random coincidence. To measure the background with each scintillator separately we turned the ^{137}Cs source sideways. For the random coincidence we added additional delay to the NaI signals ($4\mu\text{s}$ for digital TSCA output and analogous signal). This causes coincident events not to trigger the coincident unit. We have used the cesium source.

4 Analysis

4.1 General Assertion of Statistical Error

The number of decays follows a POISSON distribution due to the physical and statistical nature of the decay process. Lets assume we measure n decays in a certain energy range (channel). Then the standard deviation [6] of n is

$$s_n = \sqrt{n}. \quad (13)$$

When dealing with different measurement durations t it is more convenient to compute the event rate $R = \frac{n}{t}$. With GAUSSIAN error propagation [6] we know that the standard deviation of the event rate is given by

$$s_R = \frac{s_n}{t} = \frac{\sqrt{n}}{t}. \quad (14)$$

Here we assumed that the error of the measurement duration t is neglectable¹.

In our analysis we subtract the background event rate $R_{\text{bg}} = \frac{n_{\text{bg}}}{t_{\text{bg}}}$ from our measured event rate $R_{\text{meas}} = \frac{n}{t}$. In some cases we even have to subtract the rate of random coincidences $R_{\text{rc}} = \frac{n_{\text{rc}}}{t_{\text{rc}}}$ from our signal, i.e.

$$R = R_{\text{meas}} - R_{\text{bg}} \quad \text{and} \quad R' = R_{\text{meas}} - R_{\text{bg}} - R_{\text{rc}}. \quad (15)$$

The standard deviation of the rates on the right sides² can be calculated using (14). With GAUSSIAN error propagation we can calculate the error of our signal rates R and R'

$$s_R = \sqrt{s_{R_{\text{meas}}}^2 + s_{R_{\text{bg}}}^2} = \sqrt{\frac{n}{t^2} + \frac{n_{\text{bg}}}{t_{\text{bg}}^2}} \quad (16)$$

and

$$s_R = \sqrt{s_{R_{\text{meas}}}^2 + s_{R_{\text{bg}}}^2 + s_{R_{\text{rc}}}^2} = \sqrt{\frac{n}{t^2} + \frac{n_{\text{bg}}}{t_{\text{bg}}^2} + \frac{n_{\text{rc}}}{t_{\text{rc}}^2}} \quad (17)$$

We assume that the standard deviation of the channel C assignment, which is done by our MCAs, is given by the channel resolution. Therefore

$$s_C = 1. \quad (18)$$

We will use these standard deviations in our plots and fits.

¹In our experiment the measurement duration is given by the so called *live time* designation of the MCA readout software.

²Note that the random variables R_{meas} , R_{bg} and R_{rc} are statistically independent.

4.2 Energy Calibration

In the background revised decay spectra of ^{22}Na and ^{137}Cs are certain peaks and edges with known energies. Further information on the origin of these edges and peaks can be found in [7].

The peaks correspond to sharply defined spectral lines which are broadened by the uncertainty relation (natural line width) and the DOPPLER effect and therefore are a BREIT WIGNER curve. The width in our spectrum depends mainly on the resolution of our measurement apparatus. The signal we measure is a convolution of the BREIT WIGNER and the resolution function of our apparatus. The convolution is in good approximation a GAUSSIAN. Therefore we fit the peaks with a GAUSSIAN.

The edges correspond to the COMPTON edge. The edge could in principal be described by a Heaviside step function. The signal we measure is again the convolution of Heaviside step function and resolution function, i.e. the error function erf. Therefore we fit the COMPTON edge with an error function.

4.2.1 Inorganic Scintillator

We will now calculate the calibration function of the inorganic scintillator, the NaI scintillator.

In figure 4 we plotted the background revised event rates

$$R_{\text{NaJ,Cs}} = R_{\text{meas}} - R_{\text{bg}} \quad (19)$$

of ^{137}Cs and in figure 11 the background revised event rates of ^{22}Na . The standard deviation is given by (16). In both decay spectra we have fitted the visible peaks and edges. The χ^2/ndf is always between 0.9 and 1.3 which means that the assumptions of the fit function are good.

In Table 1 we have made an assignment of the fitted channels and the known corresponding energies [8].

Source	Energy in keV	Type	Fit #	Channel C
^{137}Cs	183	back scattering edge	1	1422 ± 3
	477	COMPTON edge	2	3284.1 ± 1.4
	662	spectral line	3	4609.2 ± 0.2
^{22}Na	341	COMPTON edge	1	2365 ± 10
	511	annihilation of e^+ and e^-	2	3583.6 ± 0.9
	1064	COMPTON edge	3	7190 ± 20
	1277	spectral line	4	8739 ± 4

Table 1: Assignment of fitted peaks and edges to the known energies [8] for the NaI scintillator.

We can now plot the energy channel pairs for the NaI scintillator, see figure 5. The relation between channel and energy should be a first order polynomial.

$$E(C) = a + b \cdot C \quad (20)$$

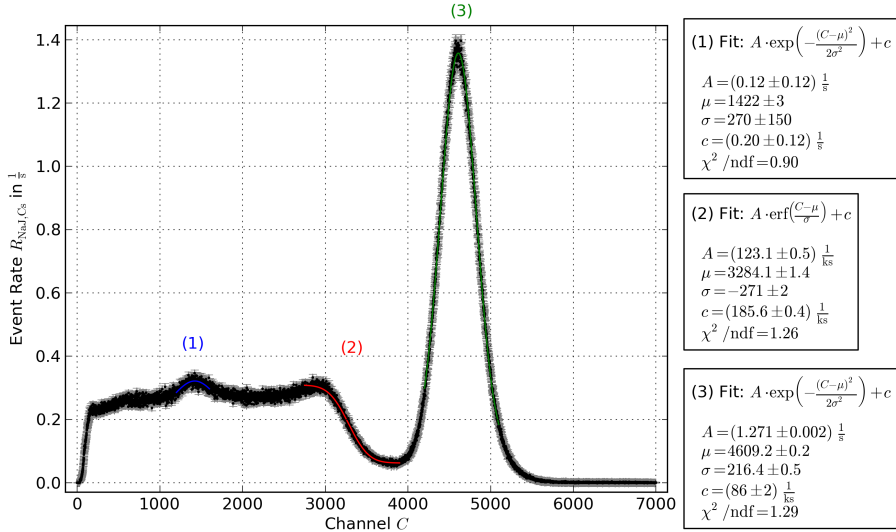


Figure 4: Background revised decay spectrum of ^{137}Cs measured with the NaI scintillator. Certain peaks and edges are fitted with the corresponding function. The gray area corresponds to the error bars. Measurement duration $t = 3600\text{s}$.

But the data points do not lay on the fit within their standard deviation what causes a very large $\chi^2/\text{ndf} = 40$. This might be caused by unknown/untreated uncertainties, which would have enlarged the standard deviation, or by more complex effects in the scintillator, so that a higher polynomial is needed.

Anyway, the fitted calibration function (20) for the NaJ scintillator is

$$E_{\text{NaI}}(C) = (-21 \pm 6) \text{ keV} + (148.8 \pm 1.3) \text{ eV} \cdot C. \quad (21)$$

4.2.2 Organic Scintillator

We have to do the same calibration as we did with the inorganic scintillator. The corresponding spectra (figure 13 and 12) and the assignments (table 6) can be found in the appendix.

In this case we only have three known energy channel pairs, which are shown in figure 6. We have fitted the same linear function (20). The resulting calibration function is

$$E_{\text{PVC}}(C) = (-152 \pm 10) \text{ keV} + (1.98 \pm 0.03) \text{ keV} \cdot C. \quad (22)$$

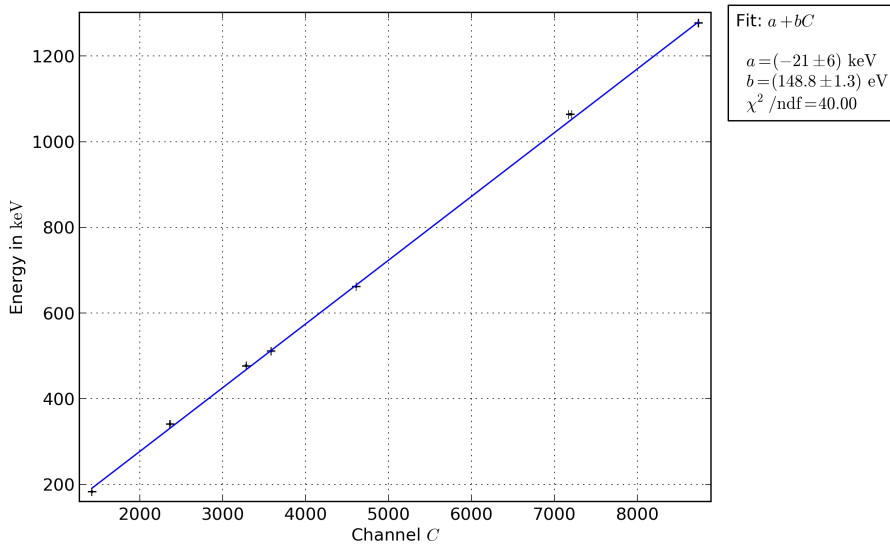


Figure 5: Energy-Channel pairs and fit for NaI scintillator. The values are taken from table 1. The x -error bars are taken from the fit results. The y -errors are assumed to be $s_E = 1$ keV.

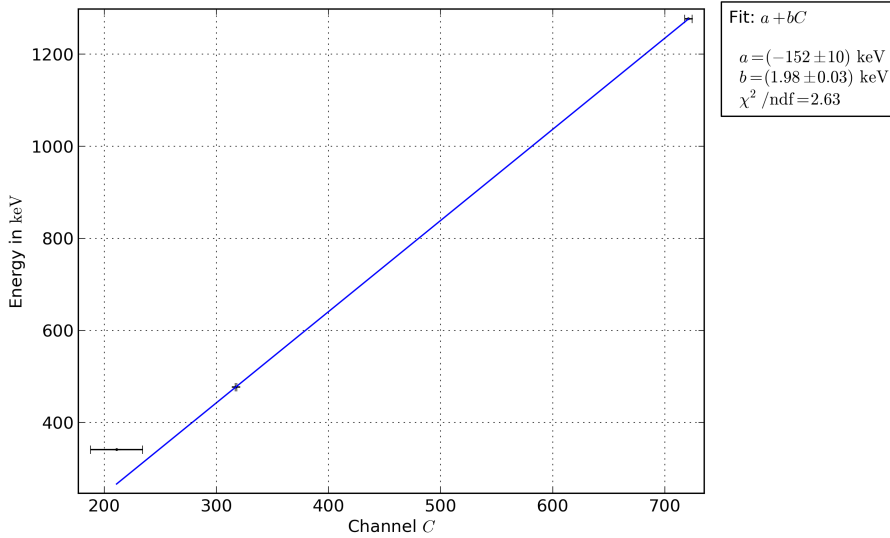


Figure 6: Energy-Channel pairs and fit for PVC scintillator. The values are taken from table 6. The x -error bars are taken from the fit results. The y -errors are assumed to be $s_E = 1$ keV.

4.3 Conservation of Energy

In the derivation of the elastic COMPTON scattering we have used the law of conservation of total energy, see (6). Now we want to verify this assumption experimentally.

We have subtracted the background and the random coincidences from the recorded spectra of both scintillator and for various angles θ

$$R = R_{\text{meas}} - R_{\text{bg}} - R_{\text{rc}}. \quad (23)$$

Here the error propagation (17) applies. One of these revised spectra is exemplarily shown in figure 7.

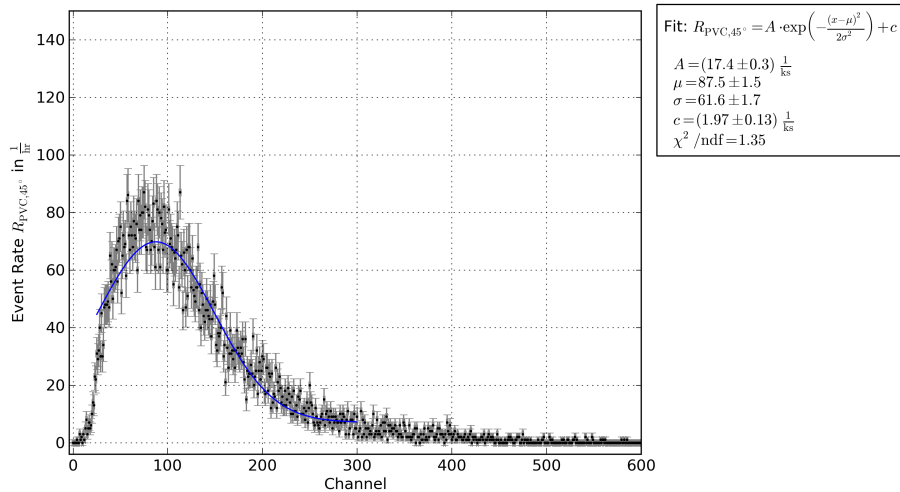


Figure 7: Electron energy spectrum (PVC scintillator) of coincident signals with $\theta = 45^\circ$.

We have fitted the peaks of the scattered electrons (PVC scintillator) and the peaks of the scattered photons (NaI scintillator) with a GAUSSIAN. The fits can be found in the appendix, see figure 14 through 31. The fit results and the corresponding energies are listed in table 2. Here we have used the calibration function for each scintillator to calculate the energies. The standard deviation of the calculated energies can be derived using GAUSSIAN error propagation

$$s_E = \sqrt{s_a^2 + C^2 s_b^2 + b^2 s_C^2} \quad (24)$$

where a and b are the calibration fit parameters from (20).

In figure 8 we have plotted all the energies of the electron and the photon for different angles. The figure also includes the sum of both energies and the theoretically expected curves (9) and (11).

From figure 8 we can say that the sum of the energies is in agreement with the theoretical constant energy within the standard deviations. Therefore we verified

$\theta/^\circ$	Channel C_{PVC}	e^- -Energy E'_e	Channel C_{NaJ}	γ -Energy E'_γ
0	8 ± 10	(0 ± 20) keV	4712 ± 12	(681 ± 9) keV
15	35 ± 2	(57 ± 11) keV	4373 ± 10	(630 ± 8) keV
30	37 ± 3	(62 ± 12) keV	4054 ± 8	(583 ± 8) keV
45	87.5 ± 1.5	(161 ± 11) keV	3198 ± 8	(455 ± 7) keV
60	129 ± 2	(243 ± 11) keV	2779 ± 7	(393 ± 7) keV
75	174.1 ± 1.4	(333 ± 11) keV	2282 ± 7	(319 ± 7) keV
90	205.6 ± 1.4	(395 ± 12) keV	2005 ± 5	(278 ± 7) keV
105	223.6 ± 1.4	(431 ± 12) keV	1819 ± 4	(250 ± 6) keV
120	234.0 ± 1.6	(452 ± 12) keV	1648 ± 4	(225 ± 6) keV

Table 2: Fit results of coincident photon and electron spectrum. The energies were calculated using the calibration functions (22) and (21).

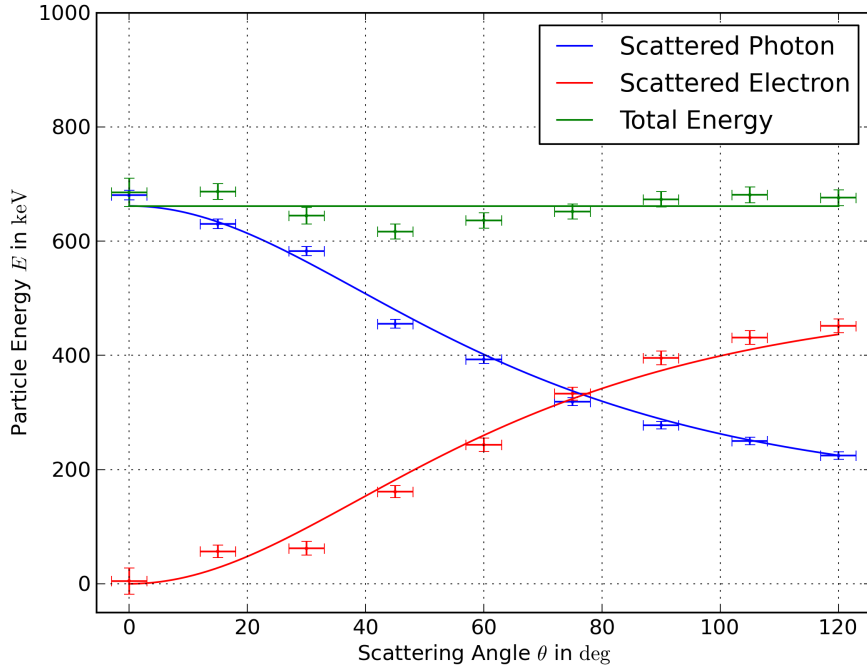


Figure 8: Measured energies of electron and photon for different angles. The values are taken from table 2. We estimated the standard deviation of the angle $s_\theta = 3^\circ$.

the conservation of energy in our measurement.

4.4 Differential Cross Section

The differential cross section $\frac{d\sigma}{d\Omega}$ is given by the KLEIN-NISHINA relation (12). To calculate the differential cross section from our measurement we have to determine the photon intensity $I(\theta)$ at a certain angle. The peaks of the scattered photons vary in width, compare figure 25 and 31. The cause might be that the apparatus resolution function is not constant over the whole energy range. An other cause is the shape of the PVC scintillator. For small measurement angles the photons can be scatter at the edge of the scintillator or in the center. Electrons at the edge have a different scattering angle compared to the ones scatter in the center. In contrast for large measurement angles the side view of the PVC scintillator is less wide, so that the scattering angle varies less. To account to this, we define the photon intensity proportional to the integral over the fitted GAUSSIAN $A \cdot \exp\left(-\frac{1}{2} \frac{(x-\mu)^2}{\sigma^2}\right)$. We define photon intensities as

$$I = A \cdot \sigma. \quad (25)$$

with its standard deviation

$$s_I = \sqrt{A^2 s_\sigma^2 + \sigma^2 s_A^2}. \quad (26)$$

A and σ are the parameters of the GAUSSIAN fits to the background and random coincidence revised spectra form 4.3.

The differential cross section should resemble the probability that the photon is scattered under an angle of θ . The probability can be estimated by the ratio $I(\theta)/I_{\text{in}}$, where $I(\theta)$ is the photon intensity scattered under an angle of θ and I_{in} is the total photon intensity emitted by the ^{137}Cs source. From our direct intensity measurement (see figure 32) we get $I_{\text{in}} =$. Furthermore we have to account to the number N of electrons or the electron density n_e . The probability of an electron being scattered is equal to the ratio of total cross section $N \cdot \sigma$ and irradiated area A of the scintillator³, see figure 9.

$$\frac{\sigma N}{A} = \frac{I}{I_{\text{in}}} \quad (27)$$

$$\Leftrightarrow \sigma = \frac{I}{I_{\text{in}}} \frac{A}{N} = \frac{I}{I_{\text{in}}} \frac{1}{\frac{N}{Ad} d} \stackrel{Ad=V}{=} \frac{I}{I_{\text{in}}} \frac{1}{n_e d} \quad (28)$$

To get the *differential* cross section, we have to derivate (28) with respect to the solid angle Ω . In our experiment we have measured the averaged spherical intensity, due to the finite dimensions of the NaI scintillator

$$I = \frac{1}{\Delta\Omega} \int_{\Omega_0}^{\Omega_1} d\Omega I(\Omega). \quad (29)$$

³Here we have made the assumption that the cross sections of all electrons do not overlap. Depending on the thickness of the scintillator, this might not be correct.

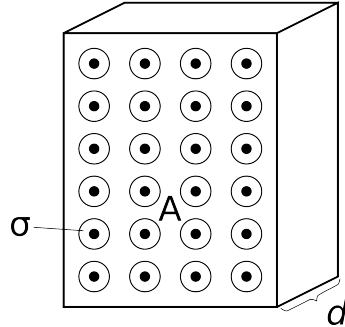


Figure 9: Illustration of the cross section (geometrical interpretation). The block represents the PVC scintillator. A is the irradiated area of the scintillator and d its thickness. The back dots represent electrons and the circles around it represent the cross section σ .

where the NaI scintillator covers the solid angle $\Delta\Omega$. The solid angle can be calculated with the radius of the NaI scintillators opening $u = (4.8 \pm 0.1)\text{cm}$ and the distance $U = (11.5 \pm 0.5)\text{cm}$ between PVC scintillator and NaI opening. The solid angle is $\Delta\Omega = \pi \cdot u^2/U^2$. Plugging this into (28) and derivating both sides, one gets

$$\frac{d\sigma}{d\Omega} = \frac{I(\theta)}{I_{\text{in}}} \frac{1}{n_e d \Delta\Omega}. \quad (30)$$

We have to account to two other effects. The NaI scintillator does not detect every single photon. The probability of a photon being detected is called efficiency ε . This means we have to divide the intensities $I(\theta)$ and I_{in} by the energy dependent efficiency. The values of ε are taken from [7] and listed in table 3.

The second effect is that the primary photons might be absorbed in the PVC scintillator before the scattering takes place or the scattered photon might be absorbed in the PVC scintillator. In both cases the calculated differential cross section would be reduced. The probability of a photon *not* being absorbed after traveling a distance x is described by $\exp(-\mu x)$ where μ is the absorption coefficient (the photon energy dependent values of μ are given in [8]). Thus the probability of a photon being absorbed is $1 - \exp(-\mu x)$. We assume that the scattering happens in the center of the PVC scintillator. The photon travels therefore half of the PVC scintillators thickness $d/2$ with the primary photon energy $E_{\text{in}} = 662\text{keV}$ and the other half with the scattered photons energy E_θ . The probability of a photon not being absorbed is then $1 - \exp(-\mu(E_{\text{in}}) \cdot d/2) \cdot \exp(-\mu(E_\theta) \cdot d/2)$.

We can now correct (30) with these two effects what leads to

$$\frac{d\sigma}{d\Omega} = \frac{I(\theta)}{I_{\text{in}}} \cdot \frac{\varepsilon(E_{\text{in}})}{\varepsilon(E_\theta)} \cdot \frac{1}{n_e d \Delta\Omega} \cdot \frac{1}{1 - e^{-\mu(E_{\text{in}}) d/2} e^{-\mu(E_\theta) d/2}}. \quad (31)$$

The standard deviation of this term can be calculated using GAUSSIAN error propagation [6]. We calculated the standard deviation using Python and the ephys

package⁴, and because the formula is rather lengthy, we will not show it here. The standard deviation of the efficiency $s_\varepsilon = 0.03$ and of the absorption coefficients $s_\mu = 0.01/\text{cm}$ are estimated from the reading precision of the graph in [7] respectively the discretization of the table in [8].

θ in $^\circ$	$I(\theta)$ in 1/hr	μ in 1/cm	ε	$\frac{d\sigma}{d\Omega}$ in mbarn
0	1450 ± 90	0.089	0.40	43 ± 14
15	1430 ± 90	0.091	0.41	41 ± 14
30	2440 ± 110	0.091	0.45	60 ± 20
45	3300 ± 300	0.098	0.51	70 ± 20
60	3240 ± 110	0.108	0.55	60 ± 20
75	2210 ± 120	0.120	0.63	36 ± 12
90	3230 ± 100	0.120	0.65	51 ± 16
105	4090 ± 130	0.120	0.70	60 ± 19
120	4840 ± 140	0.136	0.80	58 ± 18

Table 3: Summary of values used for the calculation of the differential cross section. Efficiency taken from [7] and absorption coefficients taken from [8]. 1barn = 10^{-28}m^2 .

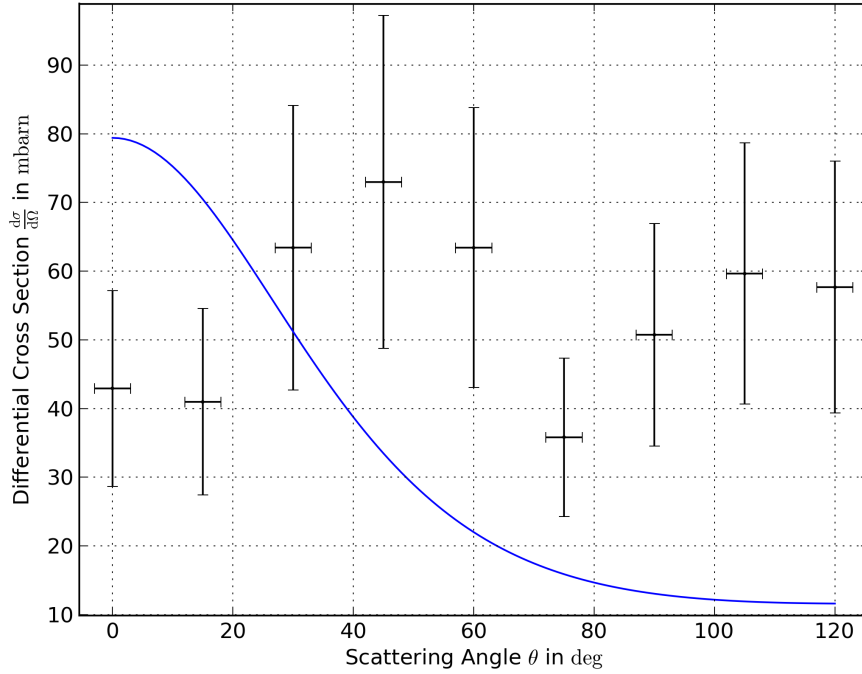


Figure 10: Comparison between measured cross section and theoretical cross section. We have estimated the uncertainty of the angle $s_\theta = 3^\circ$ from the setup equipment.

With (31) we can finally calculate the differential cross section. Table 3 summarizes this calculation. Figure 10 shows the calculated values and the values the-

⁴see <https://github.com/esel7353/ephys>, developed by Frank Sauerburger.

oretically expected from the KLEIN NISHINA formula. It is clearly visible that our values have the correct order of magnitude. Sadly the standard deviations are rather large and the values scatter around the expected values.

4.5 Discussion of Errors

The calibration fits (figure 5 and 6) and the comparison of measured differential cross section and KLEIN-NISHINA formula in figure 10 needs some discussion of errors.

The great χ^2/ndf in the calibration fits could have several reason.

- The scintillation process might not be as linear as we supposed. The photons might not be totally absorbed in the NaI scintillator. That means that they did not deport all their energy. There could be other interactions and absorptions inside the scintillator which we do not know.
- The other group in our room need absolute darkness. To ensure that the light from our equipment did not spoil their experiment, they covered our rack with a black blanket. The blanked might have turned the delay and amplification setting.
- All parts of the equipment have probably temperature dependent properties which might have changes over time.
- The digital pulses from the TSCAs were rather short compared to the analogous signals. This means that even with perfectly delayed signals the linear gate will cut parts of the analogous signals. This clearly affects our measurement.

The measured differential cross section scatters randomly around the theoretical values. Of course the possible sources of errors from above apply here as well. The measurement could be improved by prolonged measurement durations, because the peaks had only about 5 counts! An other source of errors is the assumption that the individual cross sections of the electrons do not overlap. Probably the greatest uncertainty factors are the values of μ and ε . These could be reduced by finding more readable sources.

5 Conclusion

In 4.2 we did an energy calibration for both scintillators. Our results are

$$E_{\text{NaI}}(C) = (-21 \pm 6) \text{ keV} + (148.8 \pm 1.3) \text{ eV} \cdot C. \quad (32)$$

and

$$E_{\text{PVC}}(C) = (-152 \pm 10) \text{ keV} + (1.98 \pm 0.03) \text{ keV} \cdot C. \quad (33)$$

Our first task was to verify the conservation of energy for COMPTON scattering. Figure 8 shows that we could verify the conservation of energy in our experiment. The energy of the scattered photon can therefore be calculated with

$$E'_\gamma = \frac{E_\gamma}{1 - \frac{E_\gamma}{m_e}(1 - \cos \theta)} \quad (34)$$

where E_γ is the energy of the primary photon.

Our last task was to calculate the differential cross section and compare it to the KLEIN-NISHINA formula. Figure 10 shows the result. We did show that the differential cross section is in the correct order of magnitude, but due to the larger standard deviations we can neither verify nor disproof the KLEIN-NISHINA formula.

A Appendix

A.1 Settings

Device	Delay
TSCA for NaI	1.00 (minimal setting) at $0.1 - 1.1 \mu\text{s}$
TSCA for PVC	2.20 at $1 - 11 \mu\text{s}$
Delay unit NaI	$3.25 \mu\text{s}$
Delay unit PVC	$3.75 \mu\text{s}$

Table 4: Delay settings.

Device	Coarse Gain	Fine Gain
NaI amplifier	16	6.5
PVC amplifier	8	6.0

Table 5: Amplification settings.

A.2 Energy Calibration

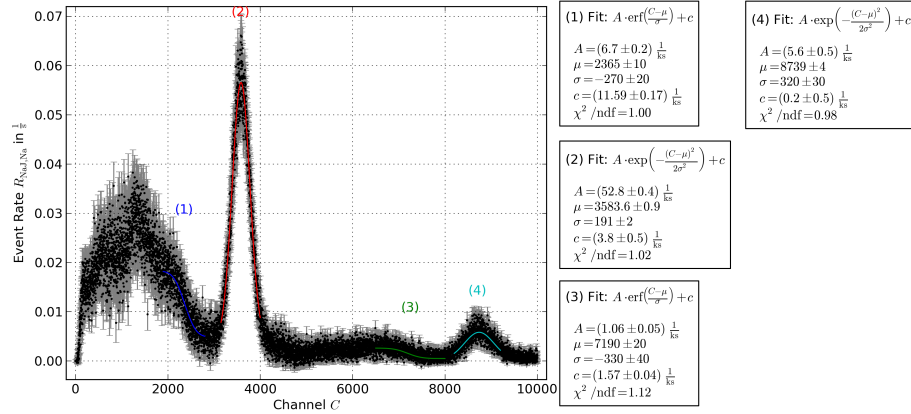


Figure 11: Background revised decay spectrum of ^{22}Na measured with the NaI scintillator. Certain peaks and edges are fitted with the corresponding function. The gray area corresponds to the error bars. Measurement duration $t = 3600\text{s}$.

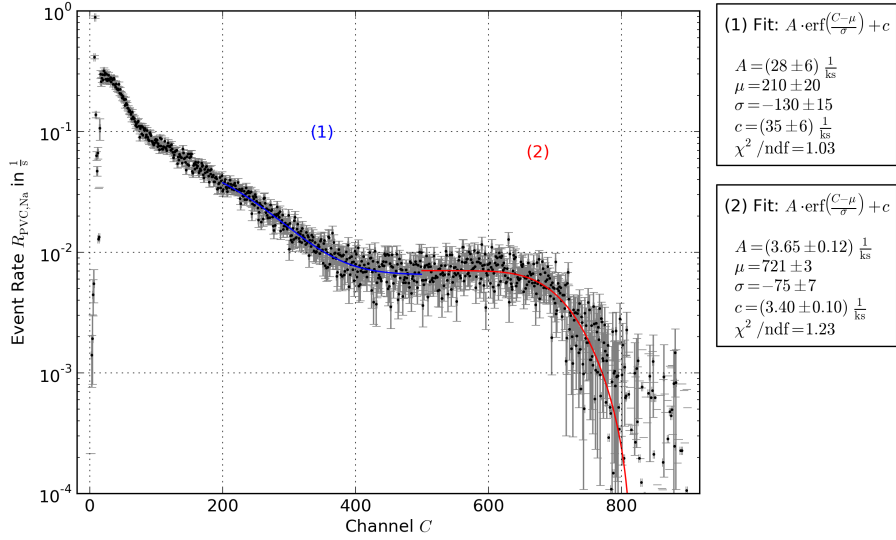


Figure 12: Background revised decay spectrum of ^{22}Na measured with the PVC scintillator. Certain peaks and edges are fitted with the corresponding function. The gray area corresponds to the error bars. Measurement duration $t = 4197.6\text{s}$.

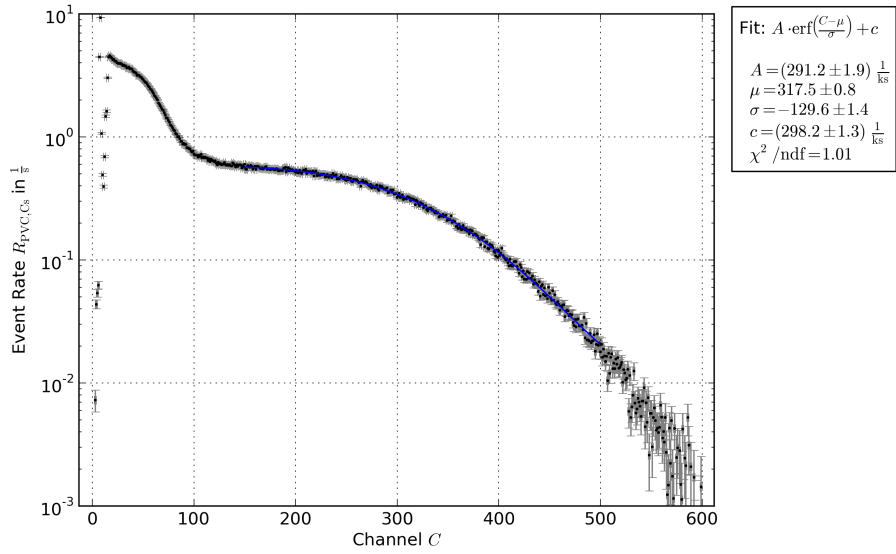


Figure 13: Background revised decay spectrum of ^{137}Cs measured with the PVC scintillator. Certain peaks and edges are fitted with the corresponding function. The gray area corresponds to the error bars. Measurement duration $t = 3600.9\text{s}$.

Source	Energy in keV	Type	Fit #	Channel C
^{137}Cs	477	COMPTON edge	1	317.5 ± 0.8
^{22}Na	341	COMPTON edge	1	210 ± 20
	1064	COMPTON edge	2	721 ± 3

Table 6: Assignment of fitted peaks and edges to the known energies [8] for the PVC scintillator.

A.3 Conservation of Energy

A.3.1 Organic Scintillator

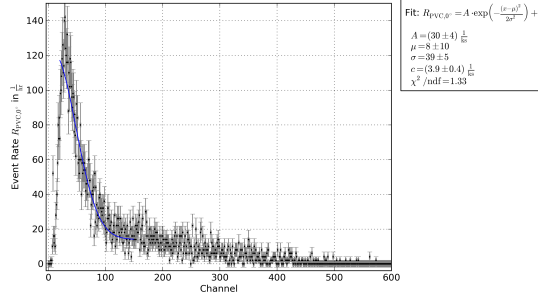


Figure 14: Electron energy spectrum (PVC scintillator) of coincident signals with $\theta = 0^\circ$. Measurement duration $t = 1880.27s$.

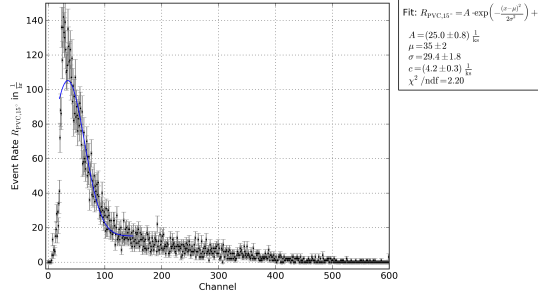


Figure 15: Electron energy spectrum (PVC scintillator) of coincident signals with $\theta = 15^\circ$. Measurement duration $t = 3600s$.

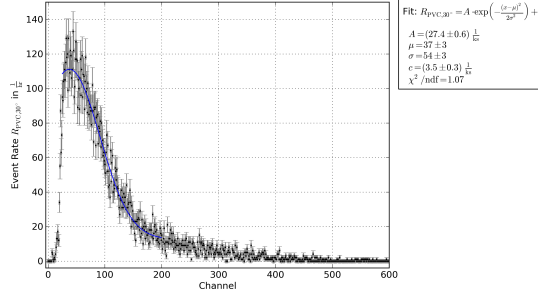


Figure 16: Electron energy spectrum (PVC scintillator) of coincident signals with $\theta = 30^\circ$. Measurement duration $t = 3699.34s$.

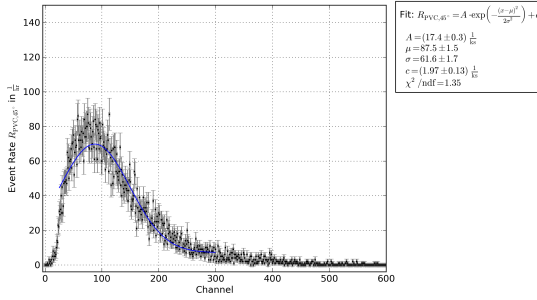


Figure 17: Electron energy spectrum (PVC scintillator) of coincident signals with $\theta = 45^\circ$. Measurement duration $t = 3600$ s.

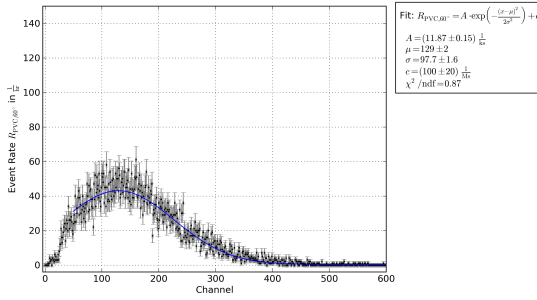


Figure 18: Electron energy spectrum (PVC scintillator) of coincident signals with $\theta = 60^\circ$. Measurement duration $t = 3600$ s.

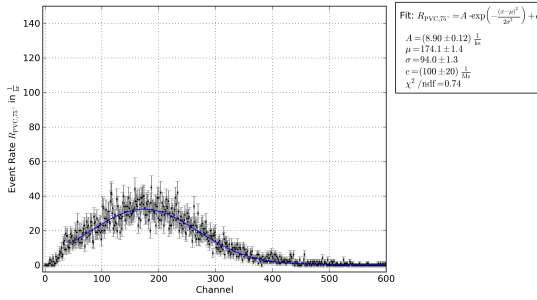


Figure 19: Electron energy spectrum (PVC scintillator) of coincident signals with $\theta = 75^\circ$. Measurement duration $t = 3600$ s.

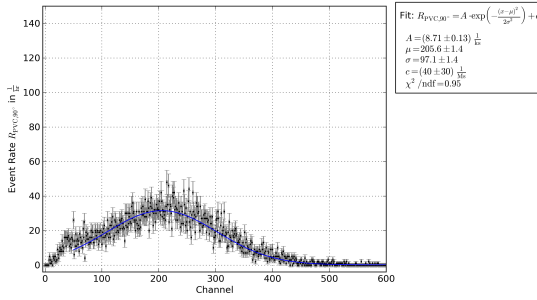


Figure 20: Electron energy spectrum (PVC scintillator) of coincident signals with $\theta = 90^\circ$. Measurement duration $t = 3600\text{s}$.

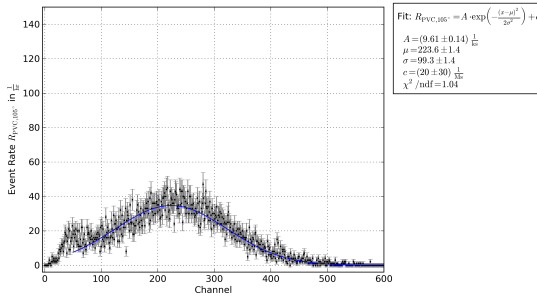


Figure 21: Electron energy spectrum (PVC scintillator) of coincident signals with $\theta = 105^\circ$. Measurement duration $t = 3600\text{s}$.

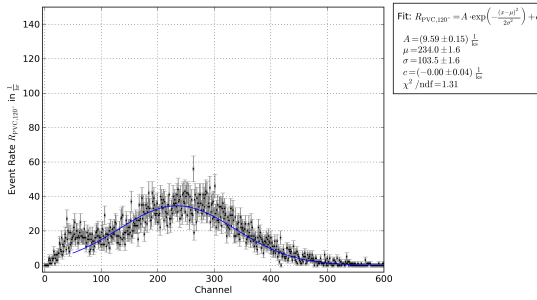


Figure 22: Electron energy spectrum (PVC scintillator) of coincident signals with $\theta = 120^\circ$. Measurement duration $t = 3600\text{s}$.

A.3.2 Anorganic Scintillator

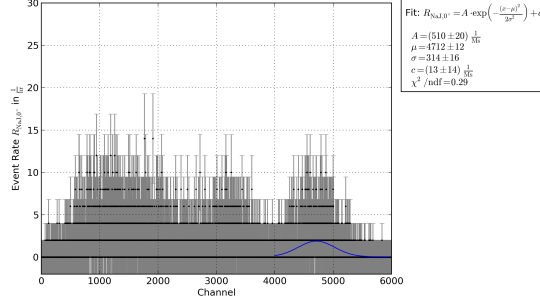


Figure 23: Photon energy spectrum (NaI scintillator) of coincident signals with $\theta = 0^\circ$. Measurement duration $t = 1800\text{s}$.

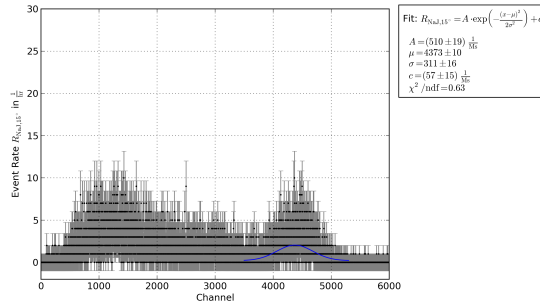


Figure 24: Photon energy spectrum (NaI scintillator) of coincident signals with $\theta = 15^\circ$. Measurement duration $t = 3600\text{s}$.

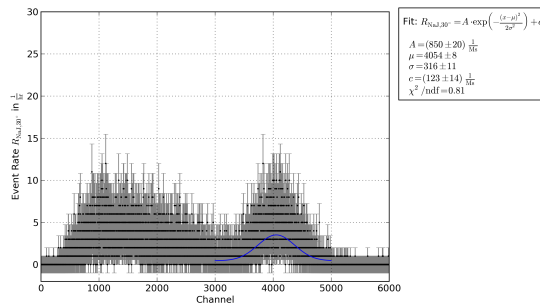


Figure 25: Photon energy spectrum (NaI scintillator) of coincident signals with $\theta = 30^\circ$. Measurement duration $t = 3600\text{s}$.

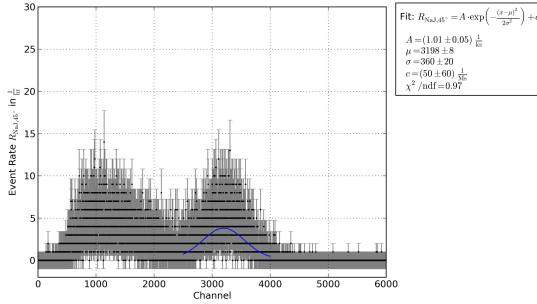


Figure 26: Photon energy spectrum (NaI scintillator) of coincident signals with $\theta = 45^\circ$. Measurement duration $t = 3600\text{s}$.

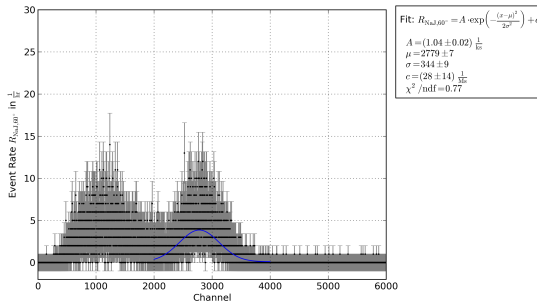


Figure 27: Photon energy spectrum (NaI scintillator) of coincident signals with $\theta = 60^\circ$. Measurement duration $t = 3600\text{s}$.

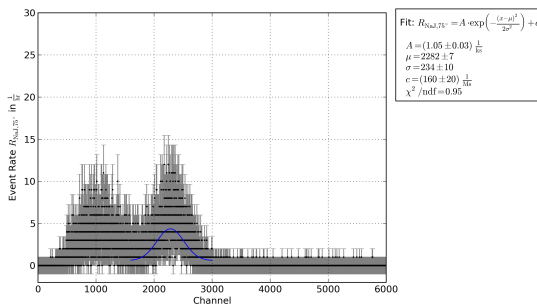


Figure 28: Photon energy spectrum (NaI scintillator) of coincident signals with $\theta = 75^\circ$. Measurement duration $t = 3600\text{s}$.

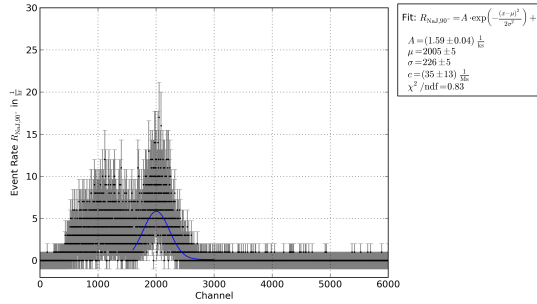


Figure 29: Photon energy spectrum (NaI scintillator) of coincident signals with $\theta = 90^\circ$. Measurement duration $t = 3600\text{s}$.

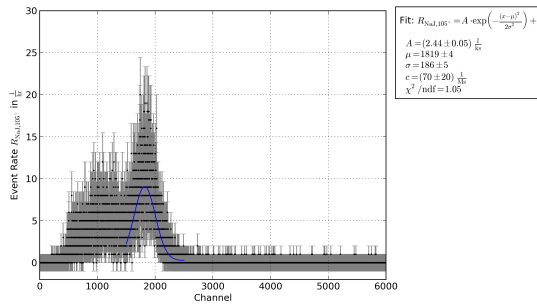


Figure 30: Photon energy spectrum (NaI scintillator) of coincident signals with $\theta = 105^\circ$. Measurement duration $t = 3600\text{s}$.

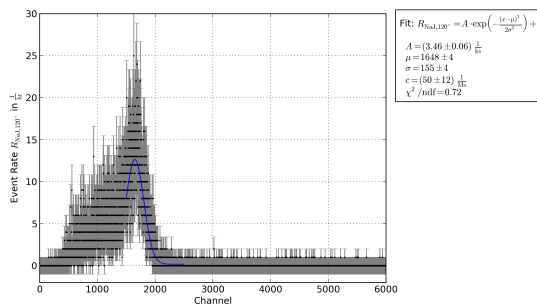


Figure 31: Photon energy spectrum (NaI scintillator) of coincident signals with $\theta = 120^\circ$. Measurement duration $t = 3600\text{s}$.

A.4 Cross Section

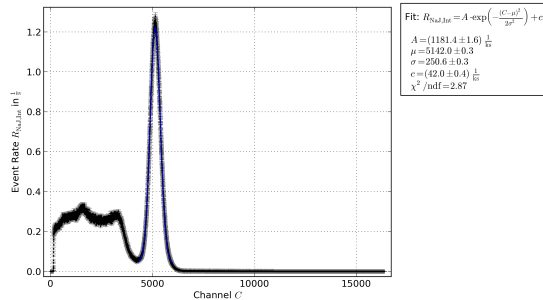


Figure 32: Direct ^{137}Cs spectrum measured with the NaI scintillator to determine the primary photon intensity. Measurement duration $t = 3600\text{s}$.

A.5 Notes

The following pages show our notes we took during the measurement.

Compton Scattering

5839

me

Kontakt:

- Verzögerungen eingestellt
- auf Orte Signale von PVC- und NaJ-Scintillatoren (nach Amp., nach Delay, nach TSC1, nach Coincidenz und Gate)

Einstellungen: TSC1: NaJ 1.0 (min) bei 0.1-0.1 μ s
PVC 2.20 bei 1-11 μ s

Delays: NaJ: $0.25 + 1 + 2 = 3.25 \mu\text{s}$
PVC: $0.25 + 0.5 + 1 + 2 = 3.75 \mu\text{s}$

- Anzahl gleichzeitige Ereignisse:

272 Ereignisse in 101.040s mit Na-Verpackung
306 in 101.161s ohne ——

- Verstärkung des NaJ einstellen (NaTest 1. TKA)

Einstellungen: is Coarse gain: 16
fine gain: 6.5
pos. bipolar

- Eichmessung: NaJ, ^{23}Na , 1h.
Natrium-Natrium.TKA

- Eichmessung: ^{23}Na , ^{137}Cs , 1h
Natrium-Caesium.TKA

- Einstellen des PVC amyo

Einstellungen: Tanne gain: 8
firn gain: 6
reg. bival

PLZ

- Eichmessung: PVC, Cs, 3600.96s
PVC-Caesium.TXT

- Untergrundmessung: PVC 57018.02s
PVC-Untergrund.TXT

- Eichmessung: PVC, Na, 4187.63s
PVC-Natrium

Drinstag

Winkelmessung / Energieerhaltung

$$(1) \theta = 0^\circ, t_{Na3} = 1800.0s \text{ ohne Fenster}$$

$$t_{PVC} = \frac{1799.5}{1880.27s}$$

$$(2) \theta = 15^\circ, t_{Na} = 3600s$$

$$t_{PVC} = 3600s$$

$$(3) \theta = 30^\circ, t_{Na} = 3600s$$

$$t_{PVC} = 3689,34s$$

$$(4) \theta = 45^\circ, t_{Na} = 3600s$$

$$t_{PVC} = 3600s$$

$$(5) \theta = 60^\circ \quad \text{---} \parallel \text{---}$$

(6) $\theta = 7,5^\circ$

— 1. —

(7) $\theta = 90^\circ$

— 11 —

• Untergrundmessung NaJ, 54000 s

Natrium-Untergrund. TK 4

72
74
8

me

Mittwoch:

Zufällige Scintillation:

• Verzögerung des NaJ um $4 \mu\text{s}$ mit 3 Decay-
schicht (analog und TSCA)

Quelle: C_S , $\theta = 0^\circ$

NaJ: NaJ-Zufall. T x T

PVC: PVC-Zufall. T x T $t = 16972.08$

• Direkte Intensität: Quelle C_S , $\theta = 0^\circ$

Differenz:

Zufällige Koincidenz: Verzögerung zwischen

NaJ: $t = 57639,533 \text{ sec}$

PVC: $t = 57653,076$

Abstand PVC-Quelle

~~PCV~~

Abstand PVC-NaJ

Durchmesser NaJ

Durchmesser Bleihloch: 16cm

Abstand PVC - Rand Bleihloch: 17cm

~~Abstand~~ Na - PVC: 11,5cm

Durchmesser Na: 4,756 cm

Dicke PVC 145cm $\pm 0,1$ cm

References

- [1] Table de radionucleides - sodium 22. Part of the additional information of the experiments manual. [Online]. Available: http://wwwhep.physik.uni-freiburg.de/fp/Versuche/FP2/FP2-4-Compton/Anhang/Na-22_tables.pdf
- [2] Table de radionucleides - cesium 137. Part of the additional information of the experiments manual. [Online]. Available: http://wwwhep.physik.uni-freiburg.de/fp/Versuche/FP2/FP2-4-Compton/Anhang/Cs-137_tables.pdf
- [3] JABBERWOK. Compton scattering. A diagram of a photon hitting a target and bouncing off. [Online]. Available: <http://en.wikipedia.org/wiki/File:Compton-scattering.svg>
- [4] W. Demtröder, *Experimentalphysik 4*. Springer-Verlag, 2014.
- [5] O. Nachtmann, *Elementarteilchenphysik - Phänomene und Konzepte*. Vieweg, 1991.
- [6] G. Cowan, *Statistical Data Analysis*. Oxford University Press, USA, 1998.
- [7] S. Flügge, *Handbuch der Physik, Band XLV*. Springer-Verlag, 1958.
- [8] M. Köhli. (2012) Versuchsanleitung fortgeschrittenen praktikum ii - compton-effekt. [Online]. Available: <http://wwwhep.physik.uni-freiburg.de/fp/Versuche/FP2/FP2-4-Compton/Anleitung.pdf>